
Direct Measurements of the Ion-Acoustic Decay Instability in a Laser-Produced, Large-Scale, Hot Plasma

The final experiment carried out on the 24-beam OMEGA laser (in collaboration with scientists from Lawrence Livermore and the University of California, Davis) involved the investigation of the ion-acoustic decay instability (IADI) in large-scale-length (~ 1 -mm), hot (~ 1 -keV) plasmas.

In the IADI, an electromagnetic wave (i.e., an incident laser beam) decays into an electron plasma wave (epw) and an ion-acoustic wave (iaw), near the critical density n_c (where the electromagnetic wave frequency equals the plasma frequency). A unique feature of this experiment was the first direct observation of the epw using collective Thomson scattering (CTS). Further, it was possible from the spectral width of the CTS signal to estimate the electron temperature T_e in the plasma, the result ($T_e = 1.5$ keV) being in reasonably good agreement with the value (1.1 keV) predicted by the two-dimensional code *SAGE*.

The IADI¹ is a fundamentally important subject in plasma physics that has been studied by numerous authors in the context of laser-plasma interactions,^{2,3} microwave experiments,⁴ and ionospheric studies.⁵ It is potentially significant in the large-scale plasmas relevant to laser fusion because anomalous electron heating can occur even when the instability is relatively weak, if the unstable volume is sufficiently large. In addition, the instability can lead to anomalous dc resistivity and a reduction in electron thermal transport, and it has an application as a critical surface diagnostic. Despite the significance of the IADI to large-scale plasmas, all previous experiments have been carried out in relatively small-scale plasmas.

In this article we present two original results: (1) the first direct observation of the epw excited by the IADI, and (2) the first study of the IADI in a plasma that approaches laser-fusion conditions, in the sense of having a density scale length of the order of 1 mm and an electron temperature T_e in excess of 1 keV. Previous observations of the epw's have been based on the second-harmonic emission, from which little can be inferred because the emission is produced by unknown pairs of

epw's, integrated in a complicated way over wave-number space and real space. In contrast, we have directly observed the epw by using the 90°, collective Thomson scattering of a UV laser (at the third harmonic of the pump) from the epw's. Because the ratio of probe frequency to electron plasma frequency is only about 3, the scattering is collective (i.e., $k_{\text{epw}}\lambda_{\text{De}}$ is small, where k_{epw} is the epw wave number and λ_{De} is the Debye length), even though the scattering angle is large. The electron temperature can then be deduced from the ion sound velocity, obtained from the measurement of the frequency at which growth is maximum at the scattering wave number.

The experiments were carried out using a large-scale (~ 1 -mm), hot (~ 1 -keV) plasma⁶ produced by the OMEGA laser in the geometry shown in Fig. 61.5. Two opposed sets of four UV beams, peaking at time $t = 1.0$ ns, were used to explode a polystyrene (CH) foil of 6- μm thickness and 600- μm diameter overcoated with 500 Å of Al. Four beams from each side were used as secondary heating beams and were incident later at $t = 1.6$ ns. The on-target laser energy was typically 50 to 60 J per beam with a pulse duration of 0.60 to 0.65 ns at a wavelength of 351 nm. One of the OMEGA beams was used as a 1.054- μm pump beam (at ω_0) to drive the IADI and timed to peak at $t = 2.2$ ns. This beam was incident through a phase plate with 3-mm cells and an $f/3.6$ lens to produce a focal spot of 210- μm diam (at half-maximum), with 36 J in the central Airy lobe, giving a maximum intensity in space and time of $\sim 1.25 \times 10^{14}$ W/cm². Another beam was attenuated and used as the $3\omega_0$ probe. A wave plate was used to rotate the (elliptical) polarization of the pump beam to the optimum angle for exciting the epw's being diagnosed. The typical plasma had a center density of 1 to 2×10^{21} cm⁻³, which was maintained within a factor of 2 at $T_e \sim 1$ keV for approximately 1 ns. The scale length was of the order of 1 mm at $t = 2.2$ ns.

The scattering geometry is shown in Fig. 61.6. The CTS signal was collected by a focusing mirror at 90° to the Thomson scattering beam and focused onto the detector system (at the opposite port), which included a 1-m spectrometer, a UV streak camera, and a CCD camera. The measured wave vector

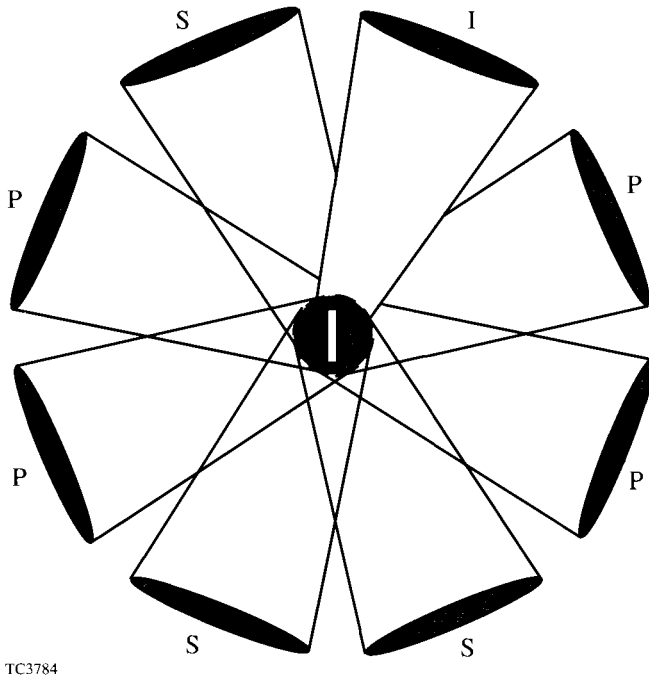


Figure 61.5

Configuration for long-scale-length plasma experiments. A plastic (CH) disk target is first irradiated by four near-normal-incidence, primary beams (P) from each side, forming an approximately spherical plasma. This plasma is then heated by four obliquely incident, secondary beams (S) from each side and one 1054-nm interaction beam (I). The interaction beam (shown shaded) is focused more tightly than the other beams.

k_{epw} was nearly parallel to the pump electric field. Simultaneously, the time-resolved, second-harmonic spectrum (through the Thomson-scattering port) was measured using a 1/3-m spectrometer, a streak camera, and another CCD camera.

Collective Thomson scattering⁷ is a three-wave process satisfying the k -matching condition $k_s = k_i \pm k_{epw}$ and the energy conservation law $\omega_s = \omega_i \pm \omega_{epw}$. (The k 's and ω 's are the wave vectors and frequencies of the three waves; the subscripts i , s , and epw refer to the incident and scattered probe beam and the electron plasma wave.) We have measured the up-shifted signal at $4\omega_0 (= \omega_i + \omega_{epw})$ to reduce the problems of incoherent harmonic emission and refraction. The scattering angle θ is given from the k -matching condition by $k_{epw}^2 = k_i^2 + k_s^2 - 2k_i k_s \cos \theta$. For the up-shifted scattering, we have $\omega_s \sim 4/3 \omega_i$ and $k_s \sim 4/3 k_i$. The geometry of the experiment selected a 90° scattering angle (Fig. 61.6) and $k_{epw} = 2.9 \times 10^5 \text{ cm}^{-1}$. At this angle the CTS signal intensity is maximum for out-of-plane polarization of the probe beam.⁷ For $T_e \sim 1 \text{ keV}$, the observed angle is close to the

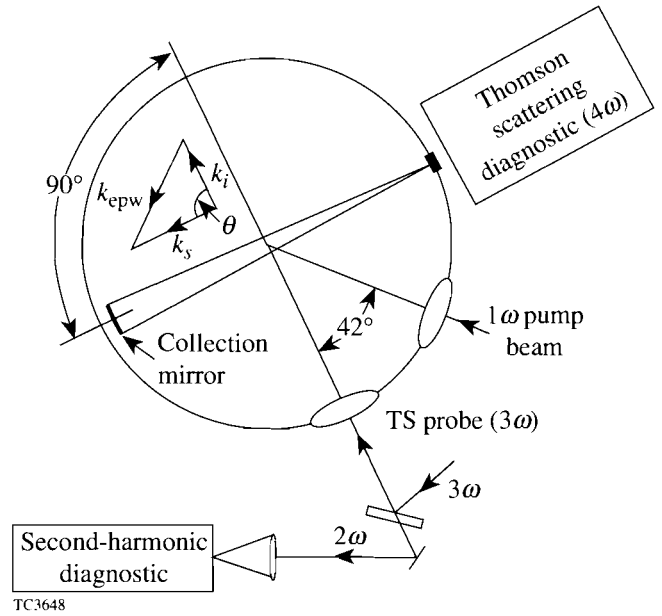


Figure 61.6

Schematic diagram of the experiment in the scattering plane. The IR pump beam is incident 6° below this plane. The initial target normal (the z axis of the simulations) is in the plane perpendicular to the scattering vector k_s and 69° below the scattering plane. It is also 69° from the pump beam. The k -matching diagram of the CTS is shown in the inset. Note that k_{epw} is nearly perpendicular to the pump laser.

optimum scattering angle of 89° for measurement of the most unstable IADI mode, which has $k_{epw} \lambda_{De} \sim 0.23$. The density at which the observed k_{epw} is resonant for the IADI depends upon T_e , becoming higher as T_e decreases.

Our experiments were guided by two-dimensional calculations using the computer code *SAGE*.⁸ Figure 61.7 shows spatial profiles of n_e , T_e , and ion temperature T_i along the center z axis at a time of 2.2 ns, corresponding to the peak of the pump beam. This timing was chosen so that the center plasma density would be slightly higher than the critical density $n_c \sim 10^{21} \text{ cm}^{-3}$ of the pump laser. When the pump laser is applied to the preformed plasma, no significant density change is predicted, but the electrons in its path are heated by classical electron-ion collisions as is shown by the hump on the right-hand side of the T_e curve. The peak value of T_e is just above 1 keV. The *SAGE* calculations indicate that 15%–70% of the pump laser energy reaches the instability region, depending on the laser intensity.

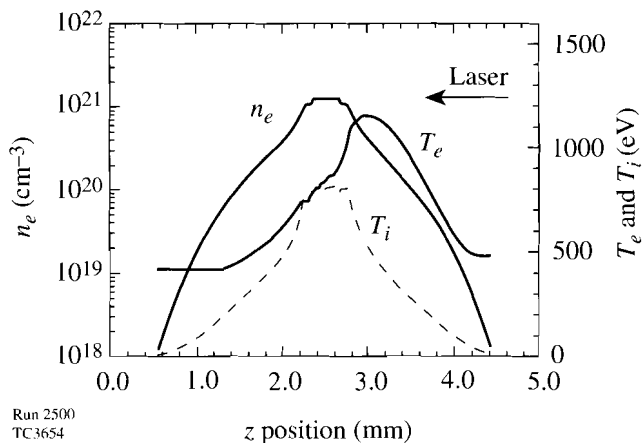


Figure 61.7
 Calculated spatial profiles of the electron density n_e and the electron and ion temperatures (T_e , T_i) at 2.2 ns. The pump laser enters from the right.

Owing to the three-dimensional nature of the experiment, some approximations were necessary. The pump beam was modeled as incident along the target normal (z), for consistency with the cylindrical symmetry about this direction assumed by *SAGE*, although the actual angle of incidence was 69° . At 2.2 ns the $0.86 n_c$ contour, at which the measured epw ($k_{\text{epw}} = 2.9 \times 10^5 \text{ cm}^{-1}$) is resonantly excited, is close to a prolate ellipsoid with diameters $560 \mu\text{m}$ along and $162 \mu\text{m}$ transverse to the z axis. Typical rays are incident at 21° to the ellipsoid normal and see flow velocities v_f of 1 to $2 \times 10^7 \text{ cm/s}$ generally directed away from the plasma center. The experimental geometry is such that $v_f \cdot k_{\text{epw}} \approx 0$.

We verified that the measured signals were caused by CTS from the IADI-excited epw as follows: (1) the $4\omega_0$ intensity decreased rapidly as the pump laser intensity decreased, and the signal disappeared when the pump was below the IADI threshold (as determined by conventional second-harmonic emission measurements); (2) when the probe beam was turned off, no $4\omega_0$ signal was observed; and (3) the $4\omega_0$ intensity varied drastically (decreased about ten times) when the probe beam polarization was changed from out-of-plane to in-plane. Moreover, the measurements discussed in the remainder of this article are all consistent with standard instability theory for a uniform plasma.¹

The experimental threshold value of the spatially averaged intensity in the instability region was estimated to be $\sim(1.4\text{--}2.8) \times 10^{12} \text{ W/cm}^2$, based on the measured threshold laser energy for a CTS signal (5 J) and taking into account the collisional attenuation and refraction as estimated by *SAGE*.

This result is in satisfactory agreement with the theoretical value⁹ of $\sim(0.8\text{--}2.3) \times 10^{12} \text{ W/cm}^2$ calculated using $T_e = 0.8 \text{ keV}$ (appropriate for a low pump intensity), taking into account the swelling at the instability region and the multiple-species ion sound theory of Ref. 10.

Figure 61.8(a) shows a CTS measurement of the time evolution of the epw spectral density function with $k_{\text{epw}} = 2.9 \times 10^5 \text{ cm}^{-1}$. A clear red shift relative to the $4\omega_0$ wavelength is evident. This Stokes peak is due to the primary IADI decay process: in these experiments, where the pump laser energy is less than 50 J, no cascade decay process¹¹ is observed. The solid curve in Fig. 61.8(b) shows the spectral density function at the time of the peak signal of Fig. 61.8(a) plotted against the normalized frequency shift $(\omega_0 - \omega_{\text{epw}})/\Omega_{\text{iaw}}$, where Ω_{iaw} is chosen to center the spectrum on a normalized shift of 1. The CTS timing is not known precisely, but Fig. 61.8(b) is presumed to correspond to 2.2 ns, the peak of the pump beam. The dashed curve gives the IADI growth rate calculated using the experimental parameters; its peak is calculated to occur at $\omega_0 - \omega_{\text{epw}} = \Omega_{\text{iaw}}$. The IADI resonance condition is thus satisfied, and the normal mode of the iaw is excited. The measured CTS spectrum is consistent with the growth-rate curve. If the pump laser intensity were instead much larger than ten times the threshold, the growth rate peak would shift to a higher frequency and the iaw frequency would increase with the laser intensity (driven mode).

We can now estimate the phase velocity of the iaw. Since the dipole approximation is valid in these experiments, the pump laser wave number is given by $k_0 \sim k_{\text{epw}} + k_{\text{iaw}} \sim 0$, so that the wave numbers k_{iaw} and k_{epw} are approximately equal in magnitude. The ion-acoustic wave frequency used for the normalization of Fig. 61.8(b) is given by

$$\Omega_{\text{iaw}} = 2\pi c \Delta\lambda / \lambda_{4\omega}^2 \approx 9 \times 10^{12} \text{ Hz},$$

where $\Delta\lambda$ is the wavelength shift of the peak of the CTS signal ($3.3 \pm 0.2 \text{ \AA}$). The phase velocity $\Omega_{\text{iaw}}/k_{\text{iaw}}$ of the iaw is then determined to be about $3 \times 10^7 \text{ cm/s}$ and may now be used to estimate the electron temperature.

The electron temperature depends on the ion-acoustic dispersion relation. To calculate this with greater accuracy, the multiple-ion nature of the plasma was included. Williams *et al.*¹⁰ have obtained fast- and slow-wave solutions for CH plasmas and have shown that the slow wave is the important one, as it is eight times less damped than the fast wave. The phase velocity of the slow wave is effectively independent of

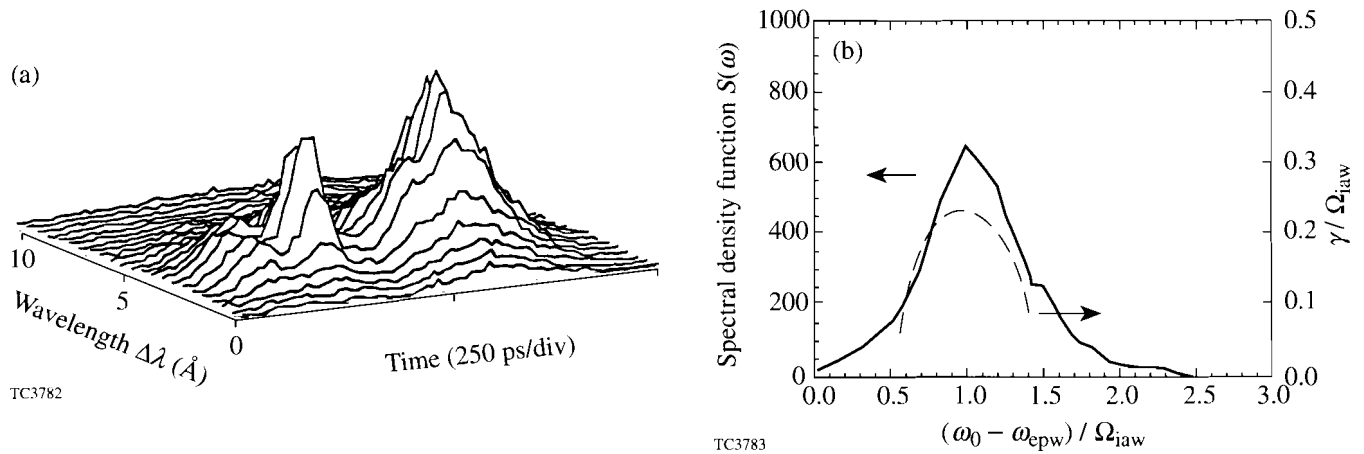


Figure 61.8

(a) Time evolution of the spectral density function of the epw (with $k_{epw} = 2.9 \times 10^5 \text{ cm}^{-1}$) measured by CTS. (b) Solid line: the spectral density function of the same epw at $t \approx 2.2 \text{ ns}$. Dashed line: the IADI growth rate calculated for a laser intensity five times threshold.

T_i in the range $0.3 < T_i/T_e < 1$, being about $0.8 (k_B T_e/M)^{1/2}$ or $1.87 \times 10^{-2} v_e$, where M is the proton mass, k_B is Boltzmann's constant, and v_e is the electron thermal velocity. The slow iaw frequency at a given wave number is thus an excellent diagnostic for T_e : from the measured peak-signal frequency shift and the scattering wave vector (known from the geometry), one immediately obtains the slow iaw velocity and hence T_e . In this experiment, the iaw phase velocity is $3 \times 10^7 \text{ cm/s}$, giving $T_e = 1.5 \text{ keV}$ and $v_e = 1.6 \times 10^9 \text{ cm/s}$. The theoretical values ($v_e = 1.4 \times 10^9 \text{ cm/s}$ and $T_e = 1.1 \text{ keV}$) given by the SAGE calculation (Fig. 61.7) are somewhat lower than the experimental values (about 13% for v_e and 27% for T_e). However, if the complicated nature of the large-scale plasma produced, the possibility of hot spots within the focal spot, and the three-dimensional nature of the experiment are all taken into account, the theoretical and experimental values are in reasonably good agreement.

Several conditions were met that enabled the diagnostic to work well:

- The scattering angle was chosen to be large to measure the most unstable epw.
- Between the thresholds for the slow-ion-wave IADI (I_{th}) and the fast-ion-wave IADI ($8 I_{th}$), only the former was significantly excited.
- The refraction of the probe beam itself was small (less than 7% for this experiment) and that of the up-shifted signal even smaller.

- The complications of plasma flow effects on the diagnostic were minimized because the detection vector ($k_{epw} = k_s - k_i$) was perpendicular to the direction of plasma expansion.
- Because this is a collective scattering, the scattering rate is much larger than that from thermal electrons, and it is relatively easy to exceed the background bremsstrahlung emissions.
- The experimental design assured that only a narrow range of densities could contribute to the observed signals.¹²

We also measured the conventional second-harmonic signal (from the coupling between two epw's) and found its threshold laser energy to be comparable to that of the CTS threshold energy, consistent with the presence of the IADI. The Stokes signal is spread over a large wavelength range and decreases gradually without a distinct peak. This finding indicates that the epw intensity is spread over a wide range of wave numbers in the large-scale plasma.

In summary, we have studied the ion-acoustic decay instability in a large-scale-length ($\sim 1\text{-mm}$), hot ($\sim 1\text{-keV}$) plasma, which is relevant to a laser fusion reactor target, and have shown that the IADI threshold is low. We have also developed a novel collective Thomson scattering diagnostic for the interaction of a $1\text{-}\mu\text{m}$ pump laser near its critical density, using the third harmonic of the interaction laser at a 90° scattering angle, and we have used this diagnostic to measure the electron plasma wave excited by the ion-acoustic decay insta-

bility near the critical density ($n_e \sim 0.86 n_c$). The frequency of the detected wave obtained from this diagnostic has been used to determine the electron temperature in the interaction region, yielding a result reasonably close to that predicted by the *SAGE* computer code.

ACKNOWLEDGMENT

This work was carried out in collaboration with K. Mizuno, B. S. Bauer, J. S. DeGroot, R. P. Drake, and B. Sleaford of the Plasma Physics Research Institute at the Lawrence Livermore National Laboratory and the University of California at Davis. We thank T. W. Johnston and E. A. Williams for many useful discussions, and W. L. Kruer and E. M. Campbell for their help and encouragement. This work was supported by the U.S. Department of Energy National Laser Users Facility at the University of Rochester, the U.S. Department of Energy Office of Inertial Confinement Fusion under Cooperative Agreement No. DE-FC03-92SF19460, and the U.S. Department of Energy under contract W-7405-ENG-48 with the Lawrence Livermore National Laboratory.

REFERENCES

1. W. L. Kruer, *The Physics of Laser Plasma Interactions*, Frontiers in Physics, Vol. 73 (Addison-Wesley, Redwood City, CA, 1988); K. Nishikawa, J. Phys. Soc. Jpn. **24**, 916 (1968); **24**, 1152 (1968).
2. C. Yamanaka *et al.*, Phys. Rev. Lett. **32**, 1038 (1974); K. Tanaka, W. Seka, L. M. Goldman, M. C. Richardson, R. W. Short, J. M. Soares, and E. A. Williams, Phys. Fluids **27**, 2187 (1984).
3. K. Mizuno, P. E. Young, W. Seka, R. Bahr, J. S. De Groot, R. P. Drake, and K. G. Estabrook, Phys. Rev. Lett. **65**, 428 (1990); K. Mizuno, R. P. Drake, P. E. Young, R. Bahr, W. Seka, and K. G. Estabrook, Phys. Fluids B **3**, 1983 (1991).

4. K. Mizuno *et al.*, Phys. Rev. Lett. **52**, 271 (1984); K. Mizuno, F. Kehl, and J. S. DeGroot, Phys. Rev. Lett. **56**, 2184 (1986).
5. D. F. DuBois, H. A. Rose, and D. Russell, Phys. Rev. Lett. **66**, 1970 (1991).
6. W. Seka, R. S. Craxton, R. E. Bahr, D. L. Brown, D. K. Bradley, P. A. Jaanimagi, B. Yaakobi, and R. Epstein, Phys. Fluids B **4**, 432 (1992).
7. J. Sheffield, *Plasma Scattering of Electromagnetic Radiation* (Academic Press, New York, 1975).
8. R. S. Craxton and R. L. McCrory, J. Appl. Phys. **56**, 108 (1984).
9. There is some uncertainty in this estimate, principally because the local electric field, which determines the IADI threshold, depends on the angle between the pump laser and the plasma density gradient at the instability region, due to the angular dependence of the swelling.
10. E. A. Williams *et al.*, submitted to Physics of Plasmas.
11. The cascade process for a fixed k_{epw} is that $\omega_{epw}^{(n)} = \omega_{epw}^{(n+1)} + \omega_{iaw}^{(n+1)}$, and $k_{epw}^{(n)} = k_{epw}^{(n+1)} + k_{iaw}^{(n+1)}$ (which indicates that

$$\left| k_{epw}^{(n)} \right| = \left| k_{epw}^{(n+1)} \right| + 1/2 \left| k_{iaw}^{(n+1)} \right|,$$

where $n = 1, 2 \dots$, and $n = 1$ is the epw excited by the primary IADI process).

12. The epw's excited at densities above $0.86 n_c$ have smaller wave numbers and cannot produce the observed wave vector by propagation. The epw's driven at densities much below $0.86 n_c$ are very strongly Landau damped.